Passive Model Reduction of Multiport Distributed Interconnects

Anestis Dounavis, *Student Member, IEEE,* Emad Gad, *Student Member, IEEE,* Ramachandra Achar, *Member, IEEE,* and Michel S. Nakhla, *Fellow, IEEE*

***Abstract*—Signal integrity analysis has become imperative for high-speed designs. In this paper, we present a new technique to advance Krylov-space-based passive model-reduction algorithms to include distributed interconnects described by telegrapher's equations. Interconnects can be lossy, coupled, and can include frequency-dependent parameters. In the proposed scheme, transmission-line subnetworks are treated with closed-form stamps obtained using matrix-exponential Padé, where the coefficients describing the model are computed *a priori* and analytically. In addition, a technique is given to guarantee that the contribution of these stamps to the modified nodal analysis formulation leads to a passive macromodel.**

***Index Terms*—Circuit simulation, distributed networks, frequency-dependent parameters, high-speed interconnects, Krylov-subspace techniques, model reduction, transmission lines.**

I. Introduction

RECENT trends in the very large scale integration (VLSI) industry toward higher operating speeds, sharper rise times, and smaller devices has made the signal integrity analysis a challenging task. The high-speed interconnect effects such as ringing, delay, distortion, crosstalk, attenuation, and reflections, if not predicted accurately at early design stages, can severely degrade the system performance. Interconnects can be found at various levels of design hierarchy, such as on-chip, packaging, multichip modules (MCMs), and printed circuit boards (PCBs). With increasing frequencies, lumped models become inaccurate and distributed quasi-TEM models based on telegrapher's equations become necessary. At even higher frequencies, distributed models with frequency-dependent *RLCG* parameters become necessary. Simulation of such models using SPICE-like nonlinear simulators suffers from mixed frequency/time difficulty as well as CPU inefficiency [1]–[19].

In [17], an efficient transmission-line model based on closed-form Padé approximation of exponential matrices is described. It computes an analytical stamp for general transmission lines based on the knowledge of its *RLCG* parameters matrices only. Extension of the same to include frequency-dependent parameters can be found in [18] and [19].

Manuscript received March 4, 2000; revised August 21, 2000. This work was supported in part by the Natural Sciences and Engineering Research Council of Canada, in part by Micronet, a Canadian Networks of Centers of Excellence on Microelectronics, in part by Communications and Information Technology Ontario, and in part by the Gennum Corporation.

The authors are with the Department of Electronics, Carleton University, Ottawa, BC, Canada K1S 5B6.

Publisher Item Identifier S 0018-9480(00)10726-4.

In this paper, we present an efficient model-reduction algorithm for simulation of networks including transmission-line equations. The proposed technique uses closed-form Padé approximation of exponential matrices described in [17]–[19]. The new technique guarantees the passivity of the reduced-order macromodel. Also, the proposed algorithm can include transmission lines described by frequency-dependent *RLCG* parameters.

The paper is organized as follows. Section II gives a background on the modified nodal analysis (MNA) formulation of networks including distributed transmission lines. Section III reviews the closed-form model for general transmission lines and derives its MNA stamp. Section IV presents the proposed reduction algorithm and the passivity preservation proof. Sections V and VI present numerical examples and the conclusion, respectively.

II. Formulation of Network Equations

A multiport linear subnetwork ϕ consisting of lumped *RLC* elements and *distributed components* can be described in the Laplace domain as

$$\left(\mathbf{G}_\phi + s\mathbf{C}_\phi + \sum_{k=1}^{N_t} \mathbf{D_k}\mathbf{Y_k}(s)\mathbf{D_k^T}\right)\mathbf{X}(s) = \mathbf{B}\mathbf{v_p}$$
$$\mathbf{i_p} = \mathbf{B^T}\mathbf{X}(s) \quad (1)$$

where

$\mathbf{X}(s) \in \Re^n$	Laplace transform of the vector of node voltages appended by independent voltage source currents, linear inductor currents, and port currents;
$\mathbf{G}_\phi, \mathbf{C}_\phi \in \Re^{n\times n}$	constant matrices describing the lumped memoryless and memory elements of the network, respectively;
$\mathbf{v_p}, \mathbf{i_p}$	port voltages and currents, respectively, p is the number of ports;
$\mathbf{B}$	$= [b_{i,j} \in \{0,-1\}]$ selector matrix that maps the port voltages into the node space of the network, where $i \in \{1,\ldots,n\}$, $j \in \{1,\ldots,p\}$, n is the total number of variables in the MNA formulation;
$\mathbf{D_k}$	$= [d_{i,j} \in \{0,1\}]$ with a maximum of one nonzero in each row or column, is a selector matrix that maps the vector

of currents entering the interconnect subnetwork k, into the node space $\Re^n$ of the network where $i \in \{1,\ldots,n\}$, $j \in \{1,\ldots,2m_k\}$, and m_k is the number of coupled conductors in the linear subnetwork k;

$\mathbf{Y_k}(s)$ admittance parameters for the interconnect subnetwork K and N_t is the number of interconnects.

The first and second terms in (1) cover the network's lumped components and the third term describes currents at subnetwork terminals and then maps them into rest of the network through the matrix $\mathbf{D_k}$. As is evident, (1) does not have a direct representation in the time domain, which makes it difficult to include with nonlinear simulators.

In this paper, we describe a new algorithm to overcome the above difficulty. The proposed method is based on the closed-form Padé model [17]–[19] for reduction of (1) to obtain a passive macromodel of the form

$$\begin{aligned}(\hat{\mathbf{M}} + s\hat{\mathbf{N}})\hat{\mathbf{X}}_\mathbf{a}(s) &= \hat{\mathbf{B}}_\mathbf{a}\mathbf{v_p} \\ \mathbf{i_p} &= \hat{\mathbf{B}}_\mathbf{a}^\mathbf{T}\hat{\mathbf{X}}_\mathbf{a}(s).\end{aligned} \tag{2}$$

It is to be noted that the advantages of obtaining the macromodel (2) are twofold: 1) it is in the form of ordinary differential equations and, hence, can be easily included in nonlinear simulators along with nonlinear components for the purpose of transient simulation and 2) the order of the macromodel in (2) is significantly smaller than that of the equations represented by the original system (1), thereby resulting in significant speed up during transient simulations.

III. Review of Closed-Form Transmission-Line Stamp

Consider an m-conductor coupled transmission line described by telegrapher's equations

$$\begin{aligned}\frac{\partial}{\partial x}\mathbf{v}(x,t) &= -\mathbf{R}\mathbf{i}(x,t) - \mathbf{L}\frac{\partial}{\partial t}\mathbf{i}(x,t) \\ \frac{\partial}{\partial x}\mathbf{i}(x,t) &= -\mathbf{G}\mathbf{v}(x,t) - \mathbf{C}\frac{\partial}{\partial t}\mathbf{v}(x,t)\end{aligned} \tag{3}$$

where $\mathbf{R}$, $\mathbf{L}$, $\mathbf{C}$, and $\mathbf{G} \in \Re^{m\times m}$ are the per-unit-length parameter matrices and are nonnegative definite symmetric matrices [1]. The coefficients $\mathbf{v}(x,t)$ and $\mathbf{i}(x,t) \in \Re^m$ represent the voltage and current vectors as a function of position x and time t. Equation (3) can be written in the Laplace domain using the exponential function as

$$\begin{bmatrix}\mathbf{V}(d,s)\\ \mathbf{I}(d,s)\end{bmatrix} = e^{\mathbf{Z}}\begin{bmatrix}\mathbf{V}(0,s)\\ \mathbf{I}(0,s)\end{bmatrix} \tag{4}$$

where

$$\begin{aligned}\mathbf{Z} &= \begin{bmatrix}\mathbf{0} & -\mathbf{a}(s)\\ -\mathbf{b}(s) & \mathbf{0}\end{bmatrix} d \\ \mathbf{a}(s) &= \mathbf{R} + s\mathbf{L} \\ \mathbf{b}(s) &= \mathbf{G} + s\mathbf{C}\end{aligned} \tag{5}$$

and d is the length of the line. The exponential matrix $e^{\mathbf{Z}}$ can be written as

$$e^{\mathbf{Z}} \approx \left[\mathbf{P}_{N,M}(\mathbf{Z})\right]^{-1}\mathbf{Q}_{N,M}(\mathbf{Z}) \tag{6}$$

where $\mathbf{P}_{N,M}(\mathbf{Z})$ and $\mathbf{Q}_{N,M}(\mathbf{Z})$ are ***polynomial matrices*** that can be expressed in terms of a closed-form Padé rational function [18]. For $M = N = n$, the Padé rational function of (6) can be represented as

$$\begin{aligned}&\left[\mathbf{P}_{n,n}(\mathbf{Z})\right]^{-1}\mathbf{Q}_{n,n}(\mathbf{Z}) \\ &\quad= \prod_{i=1}^{n/2}\left[\mathbf{P}_{n,n}(\mathbf{Z})_i\right]^{-1}\left[\mathbf{Q}_{n,n}(\mathbf{Z})_i\right] \\ &\quad= \prod_{i=1}^{n/2}\left[(a_i\mathbf{U}-\mathbf{Z})(a_i^*\mathbf{U}-\mathbf{Z})\right]^{-1}\left[(a_i\mathbf{U}+\mathbf{Z})(a_i^*\mathbf{U}+\mathbf{Z})\right]\end{aligned} \tag{7}$$

for even values of n and

$$\begin{aligned}&\left[\mathbf{P}_{n,n}(\mathbf{Z})\right]^{-1}\mathbf{Q}_{n,n}(\mathbf{Z}) \\ &\quad= \prod_{i=0}^{(n+1)/2}\left[\mathbf{P}_{n,n}(\mathbf{Z})_i\right]^{-1}\left[\mathbf{Q}_{n,n}(\mathbf{Z})_i\right] \\ &\quad= \left[a_0\mathbf{U}-\mathbf{Z}\right]^{-1}\left[a_0\mathbf{U}+\mathbf{Z}\right] \\ &\qquad\times \prod_{i=1}^{(n-1)/2}\left[(a_i\mathbf{U}-\mathbf{Z})(a_i^*\mathbf{U}-\mathbf{Z})\right]^{-1} \\ &\qquad\times \left[(a_i\mathbf{U}+\mathbf{Z})(a_i^*\mathbf{U}+\mathbf{Z})\right]\end{aligned} \tag{8}$$

for odd values of n. Here, $\mathbf{U}$ represents the unity matrix, $a_i = x_i + jy_i$ are complex roots for $i > 0$, and a_0 is a real root. The symbol * represents the complex conjugate operation. It is to be noted that $\mathbf{P}_{n,n}(\mathbf{Z})$ and $\mathbf{Q}_{n,n}(-\mathbf{Z})$ are strict Hurwitz polynomials [21]. This means that the real parts of coefficients a_0 and a_i in (7) and (8) are positive. The matrices $\mathbf{P}_{n,n}(\mathbf{Z})_i$ and $\mathbf{Q}_{n,n}(\mathbf{Z})_i$ are expressed as

$$\begin{aligned}\left[\mathbf{P}_{n,n}(\mathbf{Z})\right]_i &= \left[(a_i\mathbf{U}-\mathbf{Z})(a_i^*\mathbf{U}-\mathbf{Z})\right] \\ &= \begin{bmatrix}\mathbf{a}(s)\mathbf{b}(s)d^2+\rho_i^2\mathbf{U} & 2x_i\mathbf{a}(s)d \\ 2x_i\mathbf{b}(s)d & [\mathbf{a}(s)\mathbf{b}(s)]^Td^2+\rho_i^2\mathbf{U}\end{bmatrix} \\ \left[\mathbf{Q}_{n,n}(\mathbf{Z})\right]_i &= \left[(a_i\mathbf{U}+\mathbf{Z})(a_i^*\mathbf{U}+\mathbf{Z})\right] \\ &= \begin{bmatrix}\mathbf{a}(s)\mathbf{b}(s)d^2+\rho_i^2\mathbf{U} & -2x_i\mathbf{a}(s)d \\ -2x_i\mathbf{b}(s)d & [\mathbf{a}(s)\mathbf{b}(s)]^Td^2+\rho_i^2\mathbf{U}\end{bmatrix}\end{aligned} \tag{9}$$

for the subsections consisting of complex pole-zero pairs where $\rho_i^2 = x_i^2 + y_i^2$ and

$$\begin{aligned}\left[\mathbf{P}_{n,n}(\mathbf{Z})\right]_0 &= \left[a_0\mathbf{U}-\mathbf{Z}\right] = \begin{bmatrix}a_0\mathbf{U} & \mathbf{a}(s)d \\ \mathbf{b}(s)d & a_0\mathbf{U}\end{bmatrix} \\ \left[\mathbf{Q}_{n,n}(\mathbf{Z})\right]_0 &= \left[a_0\mathbf{U}+\mathbf{Z}\right] = \begin{bmatrix}a_0\mathbf{U} & -\mathbf{a}(s)d \\ -\mathbf{b}(s)d & a_0\mathbf{U}\end{bmatrix}\end{aligned} \tag{10}$$

for the subsection consisting of a real pole-zero pair.

It can be shown [18], [19] that a $2m$-port subnetwork whose hybrid parameters are given by the Padé rational function of (7), (8) can be described in the frequency domain by a set of

equations in the form $(\mathbf{F}+s\mathbf{K})\mathbf{X}(s)=\mathbf{J}$, which relate the voltages at the $2m$ ports. These equations can be used as a stamp representing the whole transmission line in the unified MNA formulation. The matrices $\mathbf{F}$ and $\mathbf{K}$ are given by

$$\mathbf{F}=\sum_i \psi_{\mathbf{i}}^{\mathbf{T}}\mathbf{G_i}\psi_{\mathbf{i}} \quad \mathbf{K}=\sum_i \psi_{\mathbf{i}}^{\mathbf{T}}\mathbf{C_i}\psi_{\mathbf{i}} \tag{11}$$

where $\mathbf{G_i}$ and $\mathbf{C_i}$ represent the stamps of each subsection, as shown in (12), at the bottom of this page, for the subsections described by (9) and

$$\mathbf{G_i}=\begin{bmatrix} \frac{d}{2a_0}\mathbf{G} & \mathbf{0} & \frac{d}{2a_0}\mathbf{G} & \mathbf{U} \\ \mathbf{0} & \frac{a_0}{2d}\mathbf{R}^{-1} & \frac{-a_0}{2d}\mathbf{R}^{-1} & -\mathbf{U} \\ \frac{d}{2a_0}\mathbf{G} & \frac{-a_0}{2d}\mathbf{R}^{-1} & \left(\frac{a_0}{2d}\mathbf{R}^{-1}+\frac{d}{2a_0}\mathbf{G}\right) & \mathbf{0} \\ \mathbf{U} & -\mathbf{U} & \mathbf{0} & \mathbf{0} \end{bmatrix}$$

$$\mathbf{C_i}=\begin{bmatrix} \frac{d}{2a_0}\mathbf{C} & \mathbf{0} & \frac{d}{2a_0}\mathbf{C} & \mathbf{0} \\ \mathbf{0} & \mathbf{0} & \mathbf{0} & \mathbf{0} \\ \frac{d}{2a_0}\mathbf{C} & \mathbf{0} & \frac{d}{2a_0}\mathbf{C} & \mathbf{0} \\ \mathbf{0} & \mathbf{0} & \mathbf{0} & \frac{2d}{a_0}\mathbf{L} \end{bmatrix} \tag{13}$$

for the subsection described by (10). The matrices $\psi_{\mathbf{i}}$ are selector matrices that map the block stamps $\mathbf{G_i}$ and $\mathbf{C_i}$ to the rest of the network variables space $\Re^{N_\phi}$, where N_ϕ is the total number of variables in the network including the extra state variables augmented by the stamps of transmission lines.

For the case of interconnects with frequency-dependent parameters, the Y-parameters of each subsection can also be expressed as in (11)–(13). A technique to model interconnects with frequency-dependent parameters while preserving the passivity of the Padé macromodel is described in [18] and [19].

Using the proposed stamp of the interconnect, the system of (1) can be put in the following form:

$$(\mathbf{M}+s\mathbf{N})\mathbf{X}_a(s)=\mathbf{B}_a\mathbf{v_p} \quad \mathbf{i_p}=\mathbf{B}_a^{\mathbf{T}}\mathbf{X}_a(s) \tag{14}$$

where

$$\mathbf{M}=\mathbf{G_a}+\sum_{k=1}^{N_t}\sum_i \left(\psi_{\mathbf{i}}^{\mathbf{k}}\right)^{\mathbf{T}}\mathbf{G}_{\mathbf{i}}^{\mathbf{k}}\psi_{\mathbf{i}}^{\mathbf{k}}$$
$$\mathbf{N}=\mathbf{C_a}+\sum_{k=1}^{N_t}\sum_i \left(\psi_{\mathbf{i}}^{\mathbf{k}}\right)^{\mathbf{T}}\mathbf{C}_{\mathbf{i}}^{\mathbf{k}}\psi_{\mathbf{i}}^{\mathbf{k}}. \tag{15}$$

Here, the matrices $\mathbf{G_a}$, $\mathbf{C_a}$, and $\mathbf{B_a}$ are obtained from $\mathbf{G}_\phi$, $\mathbf{C}_\phi$, and $\mathbf{B}$ by appending them by rows (and/or) columns that contain zeros to account for the extra state variables required for the stamp of the transmission line. Thus, $\mathbf{G_a}$, $\mathbf{C_a}$, and $\mathbf{B_a}$ can be expressed in the following block form:

$$\mathbf{G_a}=\begin{bmatrix}\mathbf{G}_\phi & \mathbf{0}\\ \mathbf{0} & \mathbf{0}\end{bmatrix} \quad \mathbf{C_a}=\begin{bmatrix}\mathbf{C}_\phi & \mathbf{0}\\ \mathbf{0} & \mathbf{0}\end{bmatrix} \quad \mathbf{B_a}=\begin{bmatrix}\mathbf{B}\\ \mathbf{0}\end{bmatrix} \tag{16}$$

The indexes i and k represent the ith subsection of the kth interconnect.

It should be noted that the MNA matrices described by (12) and (13) are obtained analytically in terms of per-unit-length parameters and predetermined constants given by the Padé approximation. An error criterion for selecting the order of the Padé approximation is described in [17]–[19]. In Section IV, we de-

$$\mathbf{G_i}=\begin{bmatrix} \left(\frac{x_i}{d}+\frac{\rho_i^2}{4x_id}\right)\mathbf{R}^{-1}+\frac{d}{4x_i}\mathbf{G} & \frac{-x_i}{d}\mathbf{R}^{-1} & \mathbf{0} & \frac{d}{4x_i}\mathbf{G} & \frac{\rho_i^2}{4x_id}\mathbf{R}^{-1} & \mathbf{0} & \mathbf{0} \\ \frac{-x_i}{d}\mathbf{R}^{-1} & \frac{x_i}{d}\mathbf{R}^{-1} & \mathbf{0} & \mathbf{0} & \mathbf{0} & \mathbf{U} & \mathbf{0} \\ \mathbf{0} & \mathbf{0} & \frac{x_id}{\rho_i^2}\mathbf{G} & \frac{-x_id}{\rho_i^2}\mathbf{G} & \mathbf{0} & -\mathbf{U} & \mathbf{0} \\ \frac{d}{4x_i}\mathbf{G} & \mathbf{0} & \frac{-x_id}{\rho_i^2}\mathbf{G} & \left(\frac{x_id}{\rho_i^2}+\frac{d}{4x_i}\right)\mathbf{G} & \mathbf{0} & \mathbf{0} & \mathbf{U} \\ \frac{\rho_i^2}{4x_id}\mathbf{R}^{-1} & \mathbf{0} & \mathbf{0} & \mathbf{0} & \frac{\rho_i^2}{4x_id}\mathbf{R}^{-1} & \mathbf{0} & -\mathbf{U} \\ \mathbf{0} & -\mathbf{U} & \mathbf{U} & \mathbf{0} & \mathbf{0} & \mathbf{0} & \mathbf{0} \\ \mathbf{0} & \mathbf{0} & \mathbf{0} & -\mathbf{U} & \mathbf{U} & \mathbf{0} & \mathbf{0} \end{bmatrix}$$

$$\mathbf{C_i}=\begin{bmatrix} \frac{d}{4x_i}\mathbf{C} & \mathbf{0} & \mathbf{0} & \frac{d}{4x_i}\mathbf{C} & \mathbf{0} & \mathbf{0} & \mathbf{0} \\ \mathbf{0} & \mathbf{0} & \mathbf{0} & \mathbf{0} & \mathbf{0} & \mathbf{0} & \mathbf{0} \\ \mathbf{0} & \mathbf{0} & \frac{x_id}{\rho_i^2}\mathbf{C} & \frac{-x_id}{\rho_i^2}\mathbf{C} & \mathbf{0} & \mathbf{0} & \mathbf{0} \\ \frac{d}{4x_i}\mathbf{C} & \mathbf{0} & \frac{-x_id}{\rho_i^2}\mathbf{C} & \left(\frac{x_id}{\rho_i^2}+\frac{d}{4x_i}\right)\mathbf{C} & \mathbf{0} & \mathbf{0} & \mathbf{0} \\ \mathbf{0} & \mathbf{0} & \mathbf{0} & \mathbf{0} & \mathbf{0} & \mathbf{0} & \mathbf{0} \\ \mathbf{0} & \mathbf{0} & \mathbf{0} & \mathbf{0} & \mathbf{0} & \frac{d}{x_i}\mathbf{L} & \mathbf{0} \\ \mathbf{0} & \mathbf{0} & \mathbf{0} & \mathbf{0} & \mathbf{0} & \mathbf{0} & \frac{4x_id}{\rho_i^2}\mathbf{L} \end{bmatrix} \tag{12}$$

scribe the model reduction algorithm for reducing the system described by (14).

IV. Model Reduction and Passivity Preservation

In this section, we describe a reduction algorithm for distributed interconnects based on the congruent transformation. We will also show how to include transmission lines with frequency-dependent parameters in the proposed reduction scheme. In addition, we will prove the passivity of the reduced-order macromodel.

A. Model Reduction

An orthonormal matrix $\mathbf{Q}$ is constructed using $\lfloor q/p \rfloor$ iterations of the block Arnoldi algorithm, such that [13]

$$\begin{aligned} \mathrm{colsp}(\mathbf{Q}) &= Kr(\mathbf{A},\mathbf{R},q) \\ \mathbf{Q}^T\mathbf{Q} &= \mathbf{I}_q \end{aligned} \tag{17}$$

where

$$\begin{aligned} \mathbf{A} &= -\mathbf{M^{-1}N} \\ \mathbf{R} &= \mathbf{M^{-1}B} \end{aligned} \tag{18}$$

$$\begin{aligned} Kr(\mathbf{A},\mathbf{R},q) &= \mathrm{colsp}\big[\mathbf{R},\mathbf{AR},\mathbf{A}^2\mathbf{R},\ldots,\mathbf{A}^{k-1}\mathbf{R}\big], \\ k &= \lfloor q/p \rfloor \end{aligned} \tag{19}$$

and $\mathbf{I}_q \in \Re^{q\times q}$ is the identity matrix.

Next, the matrix $\mathbf{Q}$ is used to reduce the augmented system matrices of (14) using the congruence transform

$$\hat{\mathbf{M}} = \mathbf{Q}^T\mathbf{M}\mathbf{Q} \quad \hat{\mathbf{N}} = \mathbf{Q}^T\mathbf{N}\mathbf{Q} \quad \hat{\mathbf{B}}_a = \mathbf{Q}^T\mathbf{B}_a. \tag{20}$$

The admittance matrix for the reduced system is given by

$$\hat{\mathbf{Y}}(s) = \hat{\mathbf{B}}_\mathbf{a}^\mathbf{T}(\hat{\mathbf{M}} + s\hat{\mathbf{N}})^{-1}\hat{\mathbf{B}}_\mathbf{a}. \tag{21}$$

It can be shown that the reduced-order system described by (20) and (21) preserves the first $\lfloor q/p \rfloor$ block moments. The proof of the preservation of moments is identical to the one given in [13], where the matrices $\mathbf{M}$ and $\mathbf{N}$ contain stamps of lumped components only. However, a new approach is needed here to prove that the reduced system is passive since the matrices $\mathbf{M}$ and $\mathbf{N}$ of the original system contains the stamps (11)–(13) of transmission lines.

B. Passivity Preservation

In this section, we prove that the reduced-model represented by (21) is passive. The sufficient and necessary conditions required for the reduced system of (21) to be passive are: 1) $\hat{\mathbf{Y}}(s^*) = \hat{\mathbf{Y}}^*(s)$ and 2) $\hat{\mathbf{Y}}(s)$, is a positive real matrix, i.e., $\mathbf{z}^{*\mathbf{T}}[\mathbf{Y}^\mathbf{T}(s^*) + \mathbf{Y}(s)]\mathbf{z} \geq \mathbf{0}$ for all complex values of s satisfying that $\mathrm{Re}(s) > 0$ and any arbitrary complex vector $\mathbf{z}$. The first condition is automatically satisfied since the reduced matrices $\hat{\mathbf{M}}$, $\hat{\mathbf{N}}$, and $\hat{\mathbf{B}}_a$ are all real. To show that the second condition is also satisfied, we set $\hat{\mathbf{Y}}_\mathbf{h}(s) = \hat{\mathbf{Y}}(s) + \hat{\mathbf{Y}}^\mathbf{T}(s^*)$ and then handle the quadratic form $z^{*T}\hat{\mathbf{Y}}_\mathbf{h}(s)\mathbf{z}$ by some vector algebra to obtain

$$\begin{aligned} &\mathbf{z}^{*\mathbf{T}}\hat{\mathbf{Y}}_\mathbf{h}(s)\mathbf{z} \\ &\quad= \mathbf{z}^{*\mathbf{T}}\hat{\mathbf{B}}_\mathbf{a}^\mathbf{T}\big[(\hat{\mathbf{M}}+s\hat{\mathbf{N}})^{-1} + (\hat{\mathbf{M}}+s^*\hat{\mathbf{N}})^{-\mathbf{T}}\big]\hat{\mathbf{B}}_\mathbf{a}\mathbf{z} \\ &\quad= \mathbf{z}^{*\mathbf{T}}\hat{\mathbf{B}}_\mathbf{a}^\mathbf{T}(\hat{\mathbf{M}}+s\hat{\mathbf{N}})^{-1}\big[(\hat{\mathbf{M}}+s\hat{\mathbf{N}}) + (\hat{\mathbf{M}}+s^*\hat{\mathbf{N}})^\mathbf{T}\big] \\ &\qquad\times (\hat{\mathbf{M}}+s^*\hat{\mathbf{N}})^{-\mathbf{T}}\hat{\mathbf{B}}_\mathbf{a}\mathbf{z}. \end{aligned} \tag{22}$$

Setting $\Phi = (\hat{\mathbf{M}}+s^*\hat{\mathbf{N}})^{-\mathbf{T}}\hat{\mathbf{B}}_\mathbf{a}\mathbf{z}$ and $s = \sigma + j\omega$ yields

$$\begin{aligned} \mathbf{z}^{*\mathbf{T}}\hat{\mathbf{Y}}_\mathbf{h}(s)\mathbf{z} &= \Phi^{*\mathbf{T}}\big[\hat{\mathbf{M}} + \hat{\mathbf{M}}^\mathbf{T} + \sigma(\hat{\mathbf{N}} + \hat{\mathbf{N}}^\mathbf{T})\big]\Phi \\ &= \Phi^{*\mathbf{T}}\mathbf{Q}^\mathbf{T}\big[\mathbf{M} + \mathbf{M}^\mathbf{T} + \sigma(\mathbf{N} + \mathbf{N}^\mathbf{T})\big]\mathbf{Q}\Phi \\ &= \mathbf{y}^{*\mathbf{T}}\big[\mathbf{M} + \mathbf{M}^\mathbf{T}\big]\mathbf{y} + \mathbf{y}^{*T}\big[\sigma(\mathbf{N} + \mathbf{N}^\mathbf{T})\big]\mathbf{y} \end{aligned} \tag{23}$$

where $\mathbf{y} = \mathbf{Q}\Phi$. Substituting from (15) for the matrices $\mathbf{M}$ and $\mathbf{N}$ in (23) and using the fact that $\mathbf{C}_\phi$ is symmetric yields

$$\begin{aligned} &\mathbf{z}^{*\mathbf{T}}\hat{\mathbf{Y}}_\mathbf{h}(s)\mathbf{z} \\ &\quad= \mathbf{y}^{*\mathbf{T}}\left(\begin{bmatrix} \mathbf{G}_\phi + \mathbf{G}_\phi^\mathbf{T} & \mathbf{0} \\ \mathbf{0} & \mathbf{0} \end{bmatrix}\right)\mathbf{y} + 2\mathbf{y}^{*\mathbf{T}}\sigma\left(\begin{bmatrix} \mathbf{C}_\phi & \mathbf{0} \\ \mathbf{0} & \mathbf{0} \end{bmatrix}\right)\mathbf{y} \\ &\qquad+ \mathbf{y}^{*\mathbf{T}}\left(\sum_{k=1}^{N_t}\sum_i \left(\psi_\mathbf{i}^\mathbf{k}\right)^\mathbf{T}\left(\mathbf{G}_\mathbf{i}^\mathbf{k} + \left(\mathbf{G}_\mathbf{i}^\mathbf{k}\right)^\mathbf{T}\right)\psi_\mathbf{i}^\mathbf{k}\right)\mathbf{y} \\ &\qquad+ \mathbf{y}^{*\mathbf{T}}\sigma\left(\sum_{k=1}^{N_t}\sum_i \left(\psi_\mathbf{i}^\mathbf{k}\right)^\mathbf{T}\left(\mathbf{C}_\mathbf{i}^\mathbf{k} + \left(\mathbf{C}_\mathbf{i}^\mathbf{k}\right)^\mathbf{T}\right)\psi_\mathbf{i}^\mathbf{k}\right)\mathbf{y}. \end{aligned} \tag{24}$$

Thus, to prove that the second condition is satisfied, we need to show that each one of the four quadratic forms in (24) is nonnegative. Firstly, we consider the first two quadratic forms. The matrices $\mathbf{C}_\phi$ and $\mathbf{G}_\phi + \mathbf{G}_\phi^\mathbf{T}$ can be formulated to be nonnegative definite [13]. Hence,

$$\begin{aligned} \mathbf{y}^{*\mathbf{T}}\left(\begin{bmatrix} \mathbf{G}_\phi + \mathbf{G}_\phi^\mathbf{T} & \mathbf{0} \\ \mathbf{0} & \mathbf{0} \end{bmatrix}\right)\mathbf{y} \geq 0 \\ 2\mathbf{y}^{*\mathbf{T}}\sigma\left(\begin{bmatrix} \mathbf{C}_\phi & \mathbf{0} \\ \mathbf{0} & \mathbf{0} \end{bmatrix}\right)\mathbf{y} \geq 0. \end{aligned} \tag{25}$$

On the other hand, proving that the last two quadratic forms in (24) are nonnegative requires showing that matrices $(\psi_\mathbf{i}^\mathbf{k})^\mathbf{T}(\mathbf{G}_\mathbf{i}^\mathbf{k} + (\mathbf{G}_\mathbf{i}^\mathbf{k})^\mathbf{T})\psi_\mathbf{i}^\mathbf{k}$ and $(\psi_\mathbf{i}^\mathbf{k})^\mathbf{T}(\mathbf{C}_\mathbf{i}^\mathbf{k} + (\mathbf{C}_\mathbf{i}^\mathbf{k})^\mathbf{T})\psi_\mathbf{i}^\mathbf{k}$ are nonnegative definite. These matrices are described in the form of a congruence transform of the matrices $\mathbf{G}_\mathbf{i}^\mathbf{k} + (\mathbf{G}_\mathbf{i}^\mathbf{k})^\mathbf{T}$ and $\mathbf{C}_\mathbf{i}^\mathbf{k} + (\mathbf{C}_\mathbf{i}^\mathbf{k})^\mathbf{T}$, respectively, where $\psi_\mathbf{i}^\mathbf{k}$ is used as the transformation matrix. Hence, $(\psi_\mathbf{i}^\mathbf{k})^\mathbf{T}(\mathbf{G}_\mathbf{i}^\mathbf{k} + (\mathbf{G}_\mathbf{i}^\mathbf{k})^\mathbf{T})\psi_\mathbf{i}^\mathbf{k}$ and $(\psi_\mathbf{i}^\mathbf{k})^\mathbf{T}(\mathbf{C}_\mathbf{i}^\mathbf{k} + (\mathbf{C}_\mathbf{i}^\mathbf{k})^\mathbf{T})\psi_\mathbf{i}^\mathbf{k}$ are nonnegative definite if $\mathbf{G}_\mathbf{i}^\mathbf{k} + (\mathbf{G}_\mathbf{i}^\mathbf{k})^\mathbf{T}$ and $\mathbf{C}_\mathbf{i}^\mathbf{k} + (\mathbf{C}_\mathbf{i}^\mathbf{k})^\mathbf{T}$ are nonnegative definite [22]. Thus, to complete the proof of passivity, we need to show that $\mathbf{G}_\mathbf{i}^\mathbf{k} + (\mathbf{G}_\mathbf{i}^\mathbf{k})^\mathbf{T}$ and $\mathbf{C}_\mathbf{i}^\mathbf{k} + (\mathbf{C}_\mathbf{i}^\mathbf{k})^\mathbf{T}$ are nonnegative definite. This proof is given in the following subsection through the establishment of the basic properties of the matrices $\mathbf{G}_\mathbf{i}^\mathbf{k}$ and $\mathbf{C}_\mathbf{i}^\mathbf{k}$.

1) Properties of $\mathbf{G_i}$ and $\mathbf{C_i}$ Matrices: For ease of presentation, we omitted the superscript k in $\mathbf{G}_\mathbf{i}^\mathbf{k}$ and $\mathbf{C}_\mathbf{i}^\mathbf{k}$. We only consider the case where these matrices represent a complex

pole-zero subsection, as in (12), since similar arguments can be used to treat the real pole-zero subsection of (13). Using (12), $\mathbf{G_i}$ and $\mathbf{C_i}$ can be represented as

$$\mathbf{G_i} = \begin{bmatrix} \mathbf{W_i} & \mathbf{E} \\ \mathbf{-E^T} & 0 \end{bmatrix} \quad \mathbf{C_i} = \begin{bmatrix} \mathbf{Z_i} & 0 \\ 0 & \mathbf{H_i} \end{bmatrix} \tag{26}$$

and (27), shown at the bottom of this page.

Clearly, $\mathbf{H_i}$ is symmetric nonnegative definite since it is block diagonal with symmetric nonnegative definite diagonal blocks [22]. The next two theorems are developed to show that $\mathbf{W_i}$ and $\mathbf{Z_i}$ are nonnegative definite.

Theorem 1: Let Θ be a block structured matrix that has only four nonzero block matrices located at the block entries (i,i), (i,j), (j,i), and (j,j). Assume that these four blocks are equal to $\mathbf{K}$, i.e.,

$$\Theta = \begin{bmatrix} \mathbf{0} & & \cdots & & \mathbf{0} \\ & \mathbf{K} & \cdots & \mathbf{K} & \\ & \vdots & & \vdots & \\ & \mathbf{K} & \cdots & \mathbf{K} & \\ \mathbf{0} & & \cdots & & \mathbf{0} \end{bmatrix} \tag{28}$$

where $\mathbf{K} \in \Re^{q \times q}$ is a nonnegative definite matrix. Θ is then nonnegative definite.

Proof: To simplify the proof considerably, we consider a permutated version of Θ, i.e., $\Theta_{\mathbf{P}}$, where

$$\Theta = \mathbf{P^T} \Theta_{\mathbf{P}} \mathbf{P} \tag{29}$$

and $\mathbf{P}$ is some suitable permutation matrix chosen such that

$$\Theta_{\mathbf{P}} = \begin{bmatrix} \mathbf{K} & \mathbf{K} & \mathbf{0} & \cdots & \mathbf{0} \\ \mathbf{K} & \mathbf{K} & \mathbf{0} & \cdots & \mathbf{0} \\ \mathbf{0} & \mathbf{0} & \mathbf{0} & \cdots & \mathbf{0} \\ \vdots & \vdots & \vdots & & \vdots \\ \mathbf{0} & \mathbf{0} & \mathbf{0} & \cdots & \mathbf{0} \end{bmatrix}. \tag{30}$$

$\Theta_{\mathbf{P}}$ can be expressed in terms of congruence transform as

$$\Theta_{\mathbf{P}} = \mathbf{F^T} \operatorname{diag}(\mathbf{K}, \mathbf{0}, \ldots, \mathbf{0}) \mathbf{F} \tag{31}$$

where

$$\mathbf{F} = \begin{bmatrix} \mathbf{U} & \mathbf{U} & \mathbf{0} & \cdots & \mathbf{0} \\ \mathbf{0} & \mathbf{U} & \mathbf{0} & \cdots & \mathbf{0} \\ \mathbf{0} & \mathbf{0} & \mathbf{U} & \cdots & \mathbf{0} \\ \vdots & \vdots & \vdots & & \vdots \\ \mathbf{0} & \mathbf{0} & \mathbf{0} & \cdots & \mathbf{U} \end{bmatrix} \tag{32}$$

and $\mathbf{U}$ is the unity matrix. From (29)–(32), the matrix Θ can be written in the form of the congruence transform

$$\Theta = (\mathbf{FP})^{\mathbf{T}} \operatorname{diag}(\mathbf{K}, \mathbf{0}, \ldots, \mathbf{0})(\mathbf{FP}). \tag{33}$$

Since $\mathbf{K}$ is nonnegative definite, then $\operatorname{diag}(\mathbf{K}, \mathbf{0}, \ldots, \mathbf{0})$ is also nonnegative definite. Hence, the matrix Θ is nonnegative definite since it is defined as a congruence transform of $\operatorname{diag}(\mathbf{K}, \mathbf{0}, \ldots, \mathbf{0})$ using $\mathbf{FP}$ as the transformation operator [22]. ■

$$\mathbf{W_i} = \begin{bmatrix} \left(\frac{x_i}{d} + \frac{\rho_i^2}{4x_i d}\right)\mathbf{R^{-1}} + \frac{d}{4x_i}\mathbf{G} & \frac{-x_i}{d}\mathbf{R^{-1}} & \mathbf{0} & \frac{d}{4x_i}\mathbf{G} & \frac{\rho_i^2}{4x_i d}\mathbf{R^{-1}} \\ \frac{-x_i}{d}\mathbf{R^{-1}} & \frac{x_i}{d}\mathbf{R^{-1}} & \mathbf{0} & \mathbf{0} & \mathbf{0} \\ \mathbf{0} & \mathbf{0} & \frac{x_i d}{\rho_i^2}\mathbf{G} & \frac{-x_i d}{\rho_i^2}\mathbf{G} & \mathbf{0} \\ \frac{d}{4x_i}\mathbf{G} & \mathbf{0} & \frac{-x_i d}{\rho_i^2}\mathbf{G} & \left(\frac{x_i d}{\rho_i^2} + \frac{d}{4x_i}\right)\mathbf{G} & \mathbf{0} \\ \frac{\rho_i^2}{4x_i d}\mathbf{R^{-1}} & \mathbf{0} & \mathbf{0} & \mathbf{0} & \frac{\rho_i^2}{4x_i d}\mathbf{R^{-1}} \end{bmatrix}$$

$$\mathbf{Z_i} = \begin{bmatrix} \frac{d}{4x_i}\mathbf{C} & \mathbf{0} & \mathbf{0} & \frac{d}{4x_i}\mathbf{C} & \mathbf{0} \\ \mathbf{0} & \mathbf{0} & \mathbf{0} & \mathbf{0} & \mathbf{0} \\ \mathbf{0} & \mathbf{0} & \frac{x_i d}{\rho_i^2}\mathbf{C} & \frac{-x_i d}{\rho_i^2}\mathbf{C} & \mathbf{0} \\ \frac{d}{4x_i}\mathbf{C} & \mathbf{0} & \frac{-x_i d}{\rho_i^2}\mathbf{C} & \left(\frac{x_i d}{\rho_i^2} + \frac{d}{4x_i}\right)\mathbf{C} & \mathbf{0} \\ \mathbf{0} & \mathbf{0} & \mathbf{0} & \mathbf{0} & \mathbf{0} \end{bmatrix}$$

$$\mathbf{E}^T = \begin{bmatrix} \mathbf{0} & \mathbf{U} & \mathbf{-U} & \mathbf{0} & \mathbf{0} \\ \mathbf{0} & \mathbf{0} & \mathbf{0} & \mathbf{U} & \mathbf{-U} \end{bmatrix}$$

$$\mathbf{H}_i = \begin{bmatrix} \frac{d}{x_i}\mathbf{L} & \mathbf{0} \\ \mathbf{0} & \frac{4x_i d}{\rho_i^2}\mathbf{L} \end{bmatrix} \tag{27}$$

Theorem 2: Let Ψ be a matrix that has the same structure as Θ, except that the blocks at the entries (i,j) and (j,i) are negated, i.e.,

$$\Psi = \begin{bmatrix} \mathbf{0} & & \cdots & & \mathbf{0} \\ & \mathbf{K} & \cdots & -\mathbf{K} & \\ & \vdots & & \vdots & \\ & -\mathbf{K} & \cdots & \mathbf{K} & \\ \mathbf{0} & & \cdots & & \mathbf{0} \end{bmatrix} \tag{34}$$

where $\mathbf{K} \in \Re^{q\times q}$ is a nonnegative definite matrix. Ψ is then nonnegative definite.

Proof: The proof of this theorem follows similar lines to the proof of the above theorem where, in this case, we consider the permutated matrix $\Psi_{\mathbf{P}}$ to put Ψ in the form of the congruence transform

$$\Psi = \mathbf{P^T}\Psi_{\mathbf{P}}\mathbf{P} \tag{35}$$

where $\mathbf{P}$ is some suitable permutation matrix such that

$$\Psi_{\mathbf{P}} = \begin{bmatrix} \mathbf{K} & -\mathbf{K} & \mathbf{0} & \cdots & \mathbf{0} \\ -\mathbf{K} & \mathbf{K} & \mathbf{0} & \cdots & \mathbf{0} \\ \mathbf{0} & \mathbf{0} & \mathbf{0} & \cdots & \mathbf{0} \\ \vdots & \vdots & \vdots & & \vdots \\ \mathbf{0} & \mathbf{0} & \mathbf{0} & \cdots & \mathbf{0} \end{bmatrix}. \tag{36}$$

$\Psi_{\mathbf{P}}$ can be expressed in the form

$$\Psi_{\mathbf{P}} = \mathbf{F^T}\,\mathrm{diag}(\mathbf{K},\mathbf{0},\ldots,\mathbf{0})\mathbf{F} \tag{37}$$

where

$$\mathbf{F} = \begin{bmatrix} \mathbf{U} & -\mathbf{U} & \mathbf{0} & \cdots & \mathbf{0} \\ \mathbf{0} & \mathbf{U} & \mathbf{0} & \cdots & \mathbf{0} \\ \mathbf{0} & \mathbf{0} & \mathbf{U} & \cdots & \mathbf{0} \\ \vdots & \vdots & \vdots & & \vdots \\ \mathbf{0} & \mathbf{0} & \mathbf{0} & \cdots & \mathbf{U} \end{bmatrix}. \tag{38}$$

From (35)–(38), Ψ can be written in terms of congruence transform

$$\Psi = (\mathbf{FP})^{\mathbf{T}}\,\mathrm{diag}(\mathbf{K},\mathbf{0},\ldots,\mathbf{0})(\mathbf{FP}). \tag{39}$$

Since $\mathbf{K}$ is nonnegative definite, the matrix $\mathrm{diag}(\mathbf{K},\mathbf{0},\ldots,\mathbf{0})$ is also nonnegative definite. Hence, Ψ is nonnegative definite since it is defined as congruence transform of $\mathrm{diag}(\mathbf{K},\mathbf{0},\ldots,\mathbf{0})$ using $\mathbf{FP}$ and as the transformation operator. ■

Corollary (1): The matrices $\mathbf{W_i}$ and $\mathbf{Z_i}$ in (27) are symmetric nonnegative definite.

Proof: $\mathbf{W_i}$ and $\mathbf{Z_i}$ can be written as

$$\begin{aligned} \mathbf{W_i} &= \mathbf{W_{i,1}} + \mathbf{W_{i,2}} + \mathbf{W_{i,3}} + \mathbf{W_{i,4}} \\ \mathbf{Z_i} &= \mathbf{Z_{i,1}} + \mathbf{Z_{i,2}} \end{aligned} \tag{40}$$

where

$$\mathbf{W_{i,1}} = \begin{bmatrix} \frac{\rho_i^2}{4x_i d}\mathbf{R}^{-1} & \mathbf{0} & \mathbf{0} & \mathbf{0} & \frac{\rho_i^2}{4x_i d}\mathbf{R}^{-1} \\ \mathbf{0} & \mathbf{0} & \mathbf{0} & \mathbf{0} & \mathbf{0} \\ \mathbf{0} & \mathbf{0} & \mathbf{0} & \mathbf{0} & \mathbf{0} \\ \mathbf{0} & \mathbf{0} & \mathbf{0} & \mathbf{0} & \mathbf{0} \\ \frac{\rho_i^2}{4x_i d}\mathbf{R}^{-1} & \mathbf{0} & \mathbf{0} & \mathbf{0} & \frac{\rho_i^2}{4x_i d}\mathbf{R}^{-1} \end{bmatrix}$$

$$\mathbf{W_{i,2}} = \begin{bmatrix} \frac{x_i}{d}\mathbf{R}^{-1} & \frac{-x_i}{d}\mathbf{R}^{-1} & \mathbf{0} & \mathbf{0} & \mathbf{0} \\ \frac{-x_i}{d}\mathbf{R}^{-1} & \frac{x_i}{d}\mathbf{R}^{-1} & \mathbf{0} & \mathbf{0} & \mathbf{0} \\ \mathbf{0} & \mathbf{0} & \mathbf{0} & \mathbf{0} & \mathbf{0} \\ \mathbf{0} & \mathbf{0} & \mathbf{0} & \mathbf{0} & \mathbf{0} \\ \mathbf{0} & \mathbf{0} & \mathbf{0} & \mathbf{0} & \mathbf{0} \end{bmatrix}$$

$$\mathbf{W_{i,3}} = \begin{bmatrix} \mathbf{0} & \mathbf{0} & \mathbf{0} & \mathbf{0} & \mathbf{0} \\ \mathbf{0} & \mathbf{0} & \mathbf{0} & \mathbf{0} & \mathbf{0} \\ \mathbf{0} & \mathbf{0} & \frac{x_i d}{\rho_i^2}\mathbf{G} & \frac{-x_i d}{\rho_i^2}\mathbf{G} & \mathbf{0} \\ \mathbf{0} & \mathbf{0} & \frac{-x_i d}{\rho_i^2}\mathbf{G} & \frac{x_i d}{\rho_i^2}\mathbf{G} & \mathbf{0} \\ \mathbf{0} & \mathbf{0} & \mathbf{0} & \mathbf{0} & \mathbf{0} \end{bmatrix}$$

$$\mathbf{W_{i,4}} = \begin{bmatrix} \frac{d}{4x_i}\mathbf{G} & \mathbf{0} & \mathbf{0} & \frac{d}{4x_i}\mathbf{G} & \mathbf{0} \\ \mathbf{0} & \mathbf{0} & \mathbf{0} & \mathbf{0} & \mathbf{0} \\ \mathbf{0} & \mathbf{0} & \mathbf{0} & \mathbf{0} & \mathbf{0} \\ \frac{d}{4x_i}\mathbf{G} & \mathbf{0} & \mathbf{0} & \frac{d}{4x_i}\mathbf{G} & \mathbf{0} \\ \mathbf{0} & \mathbf{0} & \mathbf{0} & \mathbf{0} & \mathbf{0} \end{bmatrix}$$

$$\mathbf{Z_{i,1}} = \begin{bmatrix} \frac{d}{4x_i}\mathbf{C} & \mathbf{0} & \mathbf{0} & \frac{d}{4x_i}\mathbf{C} & \mathbf{0} \\ \mathbf{0} & \mathbf{0} & \mathbf{0} & \mathbf{0} & \mathbf{0} \\ \mathbf{0} & \mathbf{0} & \mathbf{0} & \mathbf{0} & \mathbf{0} \\ \frac{d}{4x_i}\mathbf{C} & \mathbf{0} & \mathbf{0} & \frac{d}{4x_i}\mathbf{C} & \mathbf{0} \\ \mathbf{0} & \mathbf{0} & \mathbf{0} & \mathbf{0} & \mathbf{0} \end{bmatrix}$$

$$\mathbf{Z_{i,2}} = \begin{bmatrix} \mathbf{0} & \mathbf{0} & \mathbf{0} & \mathbf{0} & \mathbf{0} \\ \mathbf{0} & \mathbf{0} & \mathbf{0} & \mathbf{0} & \mathbf{0} \\ \mathbf{0} & \mathbf{0} & \frac{x_i d}{\rho_i^2}\mathbf{C} & \frac{-x_i d}{\rho_i^2}\mathbf{C} & \mathbf{0} \\ \mathbf{0} & \mathbf{0} & \frac{-x_i d}{\rho_i^2}\mathbf{C} & \frac{x_i d}{\rho_i^2}\mathbf{C} & \mathbf{0} \\ \mathbf{0} & \mathbf{0} & \mathbf{0} & \mathbf{0} & \mathbf{0} \end{bmatrix}. \tag{41}$$

Since the constants ρ_i^2 and x_i are positive and the per-unit-length parameter matrices $\mathbf{R}$, $\mathbf{L}$, $\mathbf{G}$, and $\mathbf{C}$ are nonnegative definite, then using theorems (1) and (2), all the block matrices in (41) are nonnegative definite. This means that $\mathbf{W_i}$ and $\mathbf{Z_i}$ are the summation of symmetric nonnegative definite matrices and, hence, they are symmetric nonnegative definite [22]. ■

Corollary (2): The matrices $\mathbf{C_i^k} + (\mathbf{C_i^k})^{\mathbf{T}}$ and $\mathbf{G_i^k} + (\mathbf{G_i^k})^{\mathbf{T}}$ are symmetric nonnegative definite.

Proof: This result can be easily deduced by noting that

$$\begin{aligned} \mathbf{C_i^k} + (\mathbf{C_i^k})^{\mathbf{T}} &= \begin{bmatrix} \mathbf{Z_i} & \mathbf{0} \\ \mathbf{0} & \mathbf{H_i} \end{bmatrix} + \begin{bmatrix} \mathbf{Z_i} & \mathbf{0} \\ \mathbf{0} & \mathbf{H_i} \end{bmatrix}^{\mathbf{T}} \\ &= \begin{bmatrix} 2\mathbf{Z_i} & \mathbf{0} \\ \mathbf{0} & 2\mathbf{H_i} \end{bmatrix} \end{aligned}$$

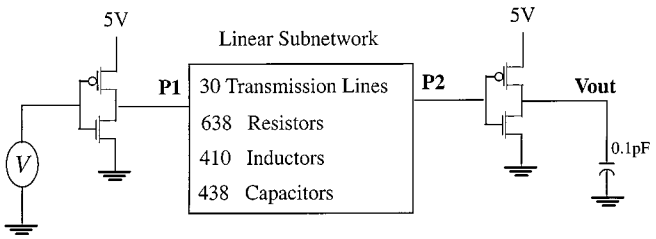

Fig. 1. Linear subnetwork circuit with nonlinear termination.

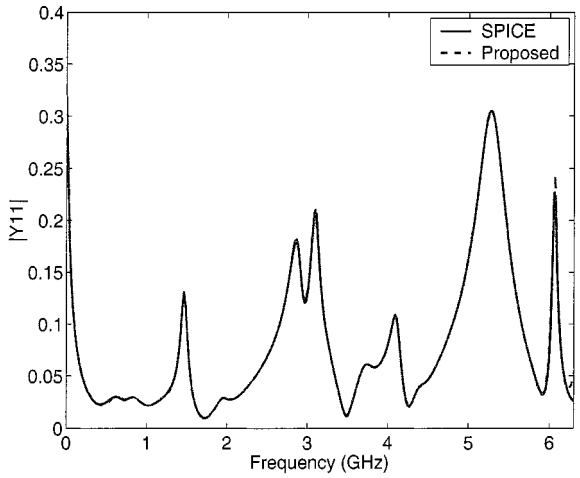

Fig. 2. Magnitude of Y_{11} of linear subnetwork for example 1.

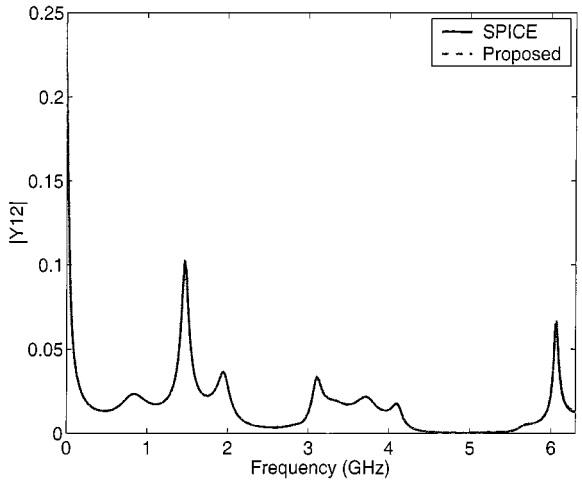

Fig. 3. Magnitude of Y_{12} of linear subnetwork for example 1.

$$\mathbf{G_i^k} + (\mathbf{G_i^k})^{\mathbf{T}} = \begin{bmatrix} \mathbf{W_i} & \mathbf{E} \\ -\mathbf{E^T} & \mathbf{0} \end{bmatrix} + \begin{bmatrix} \mathbf{W_i} & \mathbf{E} \\ -\mathbf{E^T} & \mathbf{0} \end{bmatrix}^{\mathbf{T}} = \begin{bmatrix} 2\mathbf{W_i} & \mathbf{0} \\ \mathbf{0} & \mathbf{0} \end{bmatrix} \tag{42}$$

which means that $\mathbf{C_i^k} + (\mathbf{C_i^k})^{\mathbf{T}}$ and $\mathbf{G_i^k} + (\mathbf{G_i^k})^{\mathbf{T}}$ are block diagonals with symmetric nonnegative definite diagonal blocks.■

This concludes the proof of passivity. Next, we will briefly outline the extension of the proposed passivity preservation algorithm for reduction of interconnects with frequency-independent parameters.

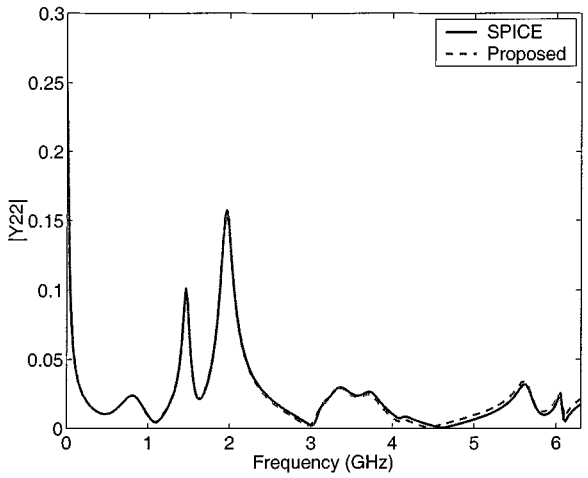

Fig. 4. Magnitude of Y_{22} of linear subnetwork for example 1.

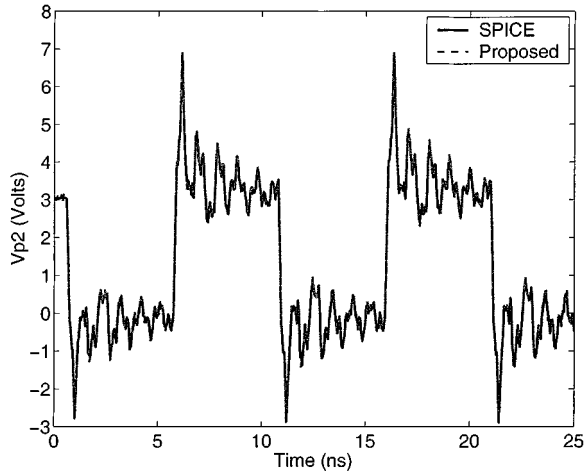

Fig. 5. Time response at output port V_{p2} for example 1.

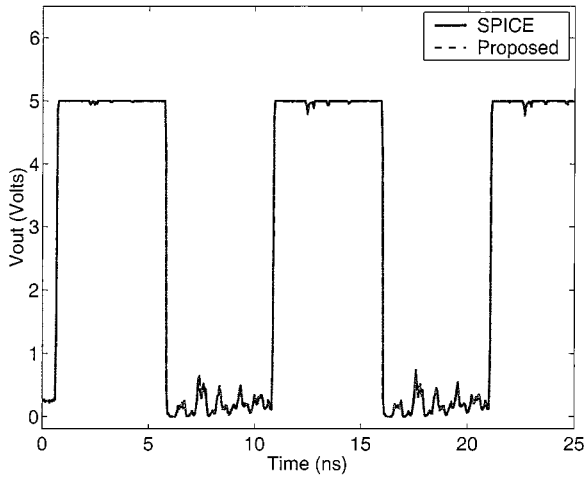

Fig. 6. Time-domain response at output node V_{out} for example 1.

TABLE I
CPU COMPARISON OF TIME RESPONSE FOR EXAMPLE 1

Proposed Method (seconds)	*Conventional lumped model (seconds)*	*Speed-up*
30	817	27

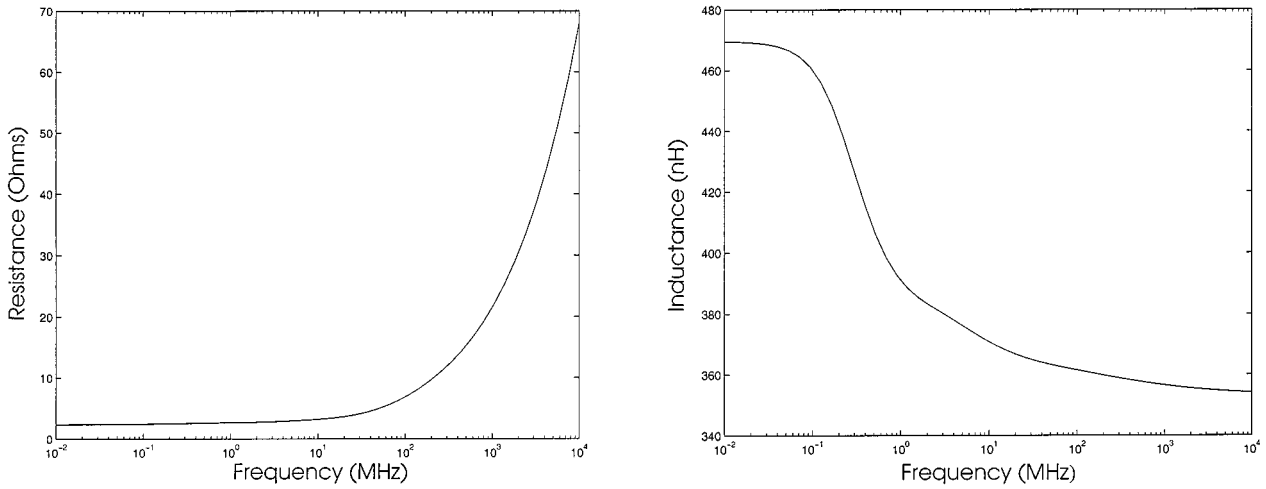

Fig. 7. R and L versus frequency for example 2.

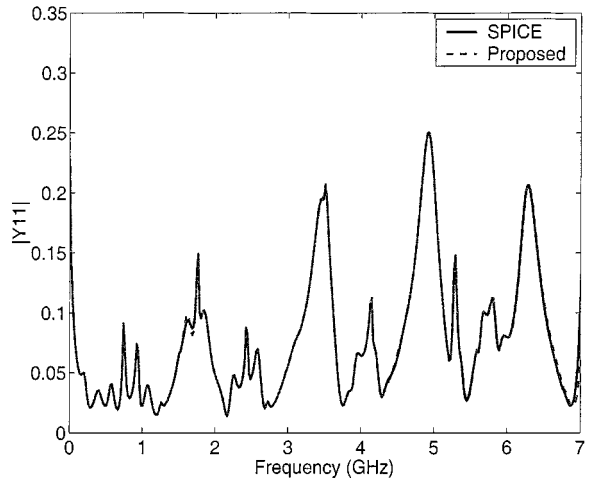

Fig. 8. Magnitude of Y_{11} of linear subnetwork for example 2.

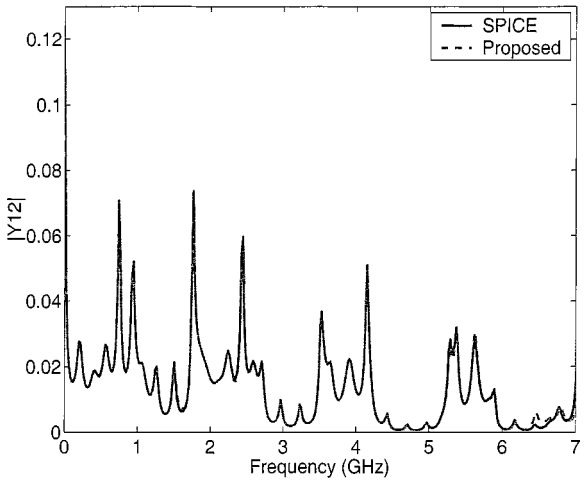

Fig. 9. Magnitude of Y_{12} of linear subnetwork for example 2.

2) Interconnects with Frequency-Dependent Parameters: In order to preserve the passivity of the reduced-order macromodel, the functions used to model the frequency-dependent parameters must be positive real. A technique to realize the frequency-dependent parameters in terms of *positive-real functions* described by *RL* components and ideal transformers can be found in [18]. The matrices $\mathbf{G_i}$ and $\mathbf{C_i}$ including transmission lines with frequency-dependent parameters can also be represented in a form similar to (26) [18]. Hence, the matrices $\mathbf{G_i}$ and $\mathbf{C_i}$ for the case of frequency-dependent parameters can also be shown to be nonnegative definite using similar proof to the one presented in Section IV-B.

V. Computational Results

Two examples are presented in this section to demonstrate the validity and efficiency of the proposed method. The second example includes interconnects with frequency-dependent parameters. The results given by the proposed method are compared with SPICE analysis. Within the context of this section, SPICE analysis refers to solving the transmission-line equations to obtain the network's frequency response or using the conventional lumped segmentation model [8] to obtain the network's time-domain response.

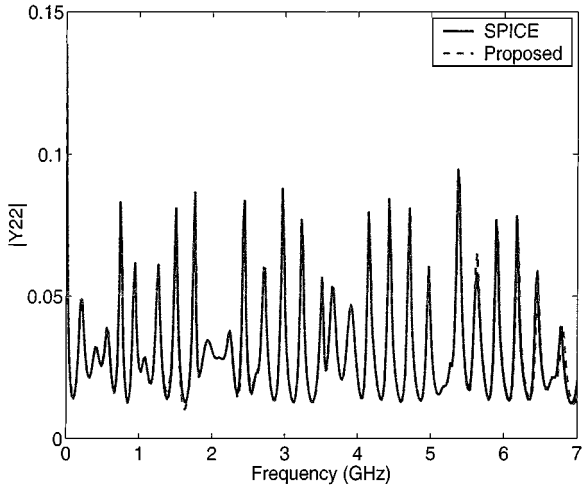

Fig. 10. Magnitude of Y_{22} of linear subnetwork for example 2.

Example 1: A two-port linear subnetwork consisting of 1516 linear components (including 30 transmission lines) with

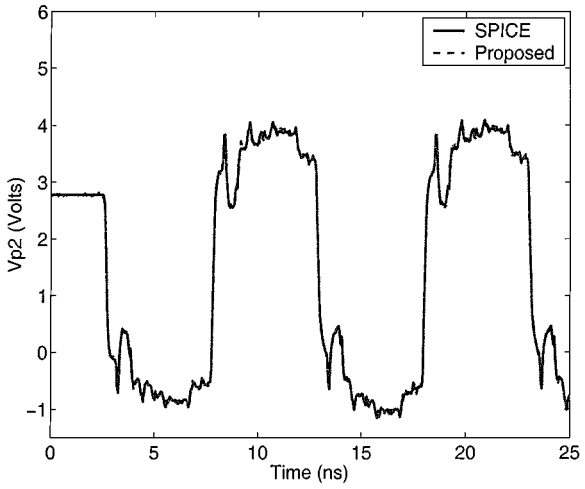

Fig. 11. Time response at output port V_{p2} for example 2.

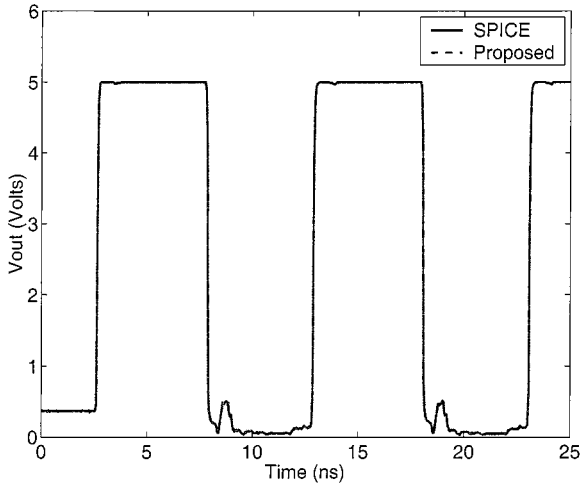

Fig. 12. Time-domain response at output node $V_{\rm out}$ for example 2.

nonlinear terminations has been considered for this example (Fig. 1). A stamp representing a rational approximation of order (5/5) was used for the transmission lines. The original set of MNA equations contained a total of 1682 variables. Using a multipoint version of the reduction algorithm of Section IV [14], the size of the reduced system obtained was 66 $\times$ 66. Figs. 2–4 show a comparison of Y-parameters of the linear subnetwork, which are obtained using SPICE analysis and the proposed method. Figs. 5 and 6 compares the time responses at two output nodes of the circuit (V_{p2} and $V_{\rm out}$), respectively. The input pulse used for this example has a rise/fall time of 0.1 ns and pulsewidth of 5 ns. The transient simulation of the reduced-order system on a Sun Ultra 20 machine required 30 s of CPU time, while the conventional lumped system required 817 s on the same machine (Table I).

Example 2: A two-port linear subnetwork consisting of 2203 linear components (*including 35 interconnects with frequency-dependent parameters*) with nonlinear terminations is considered. Fig. 7 shows the per-unit-length resistance and inductance as function of frequency. A Padé approximation (order 8/8) is used to model each interconnect. The total size of the MNA equations including the Padé interconnect stamps is 4352 variables. Performing the passive reduction scheme, a macromodel containing 184 variables is obtained. Figs. 8–10 show a comparison of Y-parameters of the linear subnetwork, which are obtained using SPICE analysis and the proposed macromodel. Figs. 11 and 12 present a comparison of time responses at output nodes V_{p2} and $V_{\rm out}$, respectively. The input pulse used for this example has a rise/fall time of 0.1 ns and pulsewidth of 5 ns. On a Sun Ultra 5 computer it takes 1.7 min to obtain the transient response with the reduced model, while the conventional lumped system requires 80.5 min (Table II).

TABLE II
CPU COMPARISON OF TIME RESPONSE FOR EXAMPLE 2

Proposed Method (minutes)	*Conventional lumped model (minutes)*	*Speed-up*
1.7	80.5	47

VI. CONCLUSION

A new algorithm has been presented in this paper to include transmission lines in passive model-reduction techniques. The transmission lines can be lossy, coupled, and can include frequency-dependent parameters. The proposed scheme uses a closed-form Padé approximation to model each transmission line. In addition, the contribution of the transmission-line stamp to the MNA equations guarantees the passivity of the reduced system.

REFERENCES

[1] C. R. Paul, *Analysis of Multiconductor Transmission Lines*. New York: Wiley, 1994.
[2] *IEEE Trans. Circuits Syst. (Special Issue)*, vol. 39, Nov. 1992.
[3] *IEEE Trans. Circuits Syst. I (Special Issue)*, vol. 47, May 2000.
[4] M. Nakhla and R. Achar, "Simulation of high-speed interconnects," *Proc. IEEE*, submitted for publication.
[5] ——, *Interconnect Modeling and Simulation*. Boca Raton, FL: CRC Press, 2000, ch. XVII, pp. 17.1–17.29.
[6] E. Chiprout and M. Nakhla, *Asymptotic Waveform Evaluation and Moment Matching for Interconnect Analysis*. Norwell, MA: Kluwer, 1993.
[7] A. Deustsch, "Electrical characteristics of interconnections for high-performance systems," *Proc. IEEE*, vol. 86, pp. 315–355, Feb. 1998.
[8] T. Dhane and D. Zutter, "Selection of lumped element models for coupled lossy transmission lines," *IEEE Trans. Computer-Aided Design*, vol. 11, pp. 959–067, July 1992.
[9] L. T. Pillage and R. A. Rohrer, "Asymptotic waveform evaluation for timing analysis," *IEEE Trans. Computer-Aided Design*, vol. 9, pp. 352–366, Apr. 1990.
[10] E. Chiprout and M. S. Nakhla, "Analysis of interconnect networks using complex frequency hopping," *IEEE Trans. Computer-Aided Design*, vol. 14, pp. 186–199, Feb. 1995.
[11] P. Feldmann and R. W. Freund, "Efficient linear circuit analysis by Padé approximation via Lanczos process," *IEEE Trans. Computer-Aided Design*, vol. 14, pp. 639–649, May 1995.
[12] L. M. Silviera, M. Kamen, I. Elfadel, and J. White, "A coordinate transformed Arnoldi algorithm for generating guaranteed stable reduced-order models for *RLC* circuits," in *ICCAD Tech. Dig.*, Nov. 1996, pp. 2288–2294.
[13] A. Odabasioglu, M. Celik, and L. T. Pilleggi, "PRIMA: Passive reduced-order interconnect macromodeling algorithm," *IEEE Trans. Computer-Aided Design*, vol. 17, Aug. 1998.
[14] I. M. Elfadel and D. D. Ling, "A block rational Arnoldi algorithm for multipoint passive model order reduction for multiport *RLC* networks," in *Proc. IEEE/ACM ICCAD*, 1997, pp. 66–71.
[15] Q. Yu, J. L. Wang, and E. Kuh, "Passive multipoint moment matching model order reduction algorithm on multiport interconnect networks," *IEEE Trans. Circuits Syst. I*, vol. 46, pp. 140–160, Jan. 1999.

[16] E. S. Kuh and J. M. L. Wang, "Recent development in interconnect analysis and simulation based on distributed models of transmission lines," in *European Circuit Theory and Design Conf.*, 1999, pp. 421–424.
[17] A. Dounavis, X. Li, M. Nakhla, and R. Achar, "Passive closed-loop transmission line model for general purpose circuit simulators," *IEEE Trans. Microwave Theory Tech.*, vol. 47, pp. 2450–2459, Dec. 1999.
[18] A. Dounavis, R. Achar, and M. Nakhla, "Efficient passive circuit models for distributed networks with frequency-dependent parameters," *IEEE Trans. Comp. Packag. Technol.*, vol. 23, pp. 382–392, Aug. 2000.
[19] A. Dounavis, "Time domain macromodels for high speed interconnects," M.Eng. thesis , Dept. Electron., Carleton Univ., Ottawa, ON, Canada, 2000.
[20] J. Vlach and K. Singhal, *Computer Methods for Circuit Analysis and Design*. New York: Van Nostrand, 1983.
[21] U. S. Pillai, *Spectrum Estimation and System Identification*. Berlin, Germany: Springer-Verlag, 1993.
[22] D. A. Harville, *Matrix Algebra from a Statistician's Perspective*. Berlin, Germany: Springer-Verlag, 1997.

Anestis Dounavis (S'95) was born in Montreal, PQ, Canada, on January 10, 1971. He received the B.Eng. degree from McGill University, Montreal, PQ, Canada, in 1995, the M.Eng. degree from Carleton University, Ottawa, ON, Canada, in 2000., and is currently working toward the Ph.D. degree in electronics at Carleton University.

His research interests include computer-aided design of VLSI systems, high-frequency interconnects, and numerical algorithms.

Mr. Dounavis was the recipient of the University Medal for his Master's thesis on time-domain macromodeling of high-speed interconnects.

Emad Gad (S'99) was born in 1969. He received the B.E. degree from Alexandria University, Alexandria, Egypt, in 1991, the M.E. degree from Cairo University, Cairo, Egypt in 1997, and is currently working toward the Ph.D. degree on developing model reduction algorithms for efficient simulation of linear and nonlinear circuits at Carleton University, Ottawa, ON, Canada.

His main research interests are circuit simulation, numerical algorithms, and learning theory.

Mr. Gad was the recipient of the 1999–2000 Ontario Graduate Scholarship in Science and Technology, the 1999 Ontario Graduate Students Scholarship, and the 2000–2001 Ontario Graduate Scholarship.

Ramachandra Achar (S'95–M'99) received the B.Eng. degree in electronics engineering from Bangalore University, Bangalore, India, in 1990, the M.Eng. degree in microelectronics from the Birla Institute of Technology and Science, Pilani, India, in 1992, and the Ph.D. degree from Carleton University, Ottawa, ON, Canada, in 1998.

During the summer of 1995, he was with the T. J. Watson Research Center, IBM, New York, NY, where he was involved with high-speed interconnect analysis. In 1992, he was a graduate trainee at the Central Electronics Engineering Research Institute, Pilani, India, and was also previously with Larsen and Toubro Engineers Ltd., Mysore, India, and the Indian Institute of Science, Bangalore, India, as an Research and Development Engineer. From 1998 to 2000, he was a Research Engineer with the Computer-Aided Engineering Group at Carleton University. He is currently an Assistant Professor in the Department of Electronics, Carleton University. His research interests include modeling and simulation of high-speed interconnects, numerical algorithms, and development of computer-aided design tools for high-frequency circuit analysis.

Dr. Achar was the recipient of the University Medal for his doctoral work on high-speed VLSI interconnect analysis. He has also received the 2000 Natural Science and Engineering Research Council Doctoral Award, the 1997 Strategic Microelectronics Corporation Award, the 1996 Canadian Microelectronics Corporation Award, and the 1998 Best Student Paper Award presented at the Micronet (a Canadian network of centers of excellence on microelectronics) Annual Workshop.

Michel S. Nakhla (S'73–M'75–SM'88–F'98) received the M.Eng. and Ph.D. degrees in electrical engineering from Waterloo University, Waterloo, ON, Canada, in 1973 and 1975, respectively.

From 1976 to 1988, he was with Bell-Northern Research (currently Nortel Networks), as the Senior Manager of the Computer-Aided Engineering Group. In 1988, he joined Carleton University, Ottawa, ON, Canada, where he is currently the Holder of the Computer Aided Engineering Senior Industrial Chair, established by Bell-Northern Research and the Natural Sciences and Engineering Research Council of Canada. He is also currently a Professor of electrical engineering, and founder of the High-Speed Computer-Aided Design (CAD) Research Group. He is a technical consultant for several industrial organizations and the principal investigator for several major sponsored research projects. His research interests include CAD of VLSI and microwave circuits, modeling and simulation of high-speed interconnects, nonlinear circuits, multidisciplinary optimization, thermal and electromagnetic (EM) emission analysis, noise analysis, mixed EM/circuit simulation, wavelets, and neural networks.